

# Secondary stars in CVs – the observational picture

K. Beuermann <sup>a 1</sup>

<sup>a</sup> *Universitäts-Sternwarte Göttingen  
Geismarlandstr. 11, 37083 Göttingen, Germany*

## Abstract

Recent theoretical and observational progress has substantially improved the definition of the lower main sequence and established a new basis for a comparison of main sequence stars and the secondaries in CVs. The evolutionary sequences of Kolb & Baraffe [1999] imply that the secondaries in many CVs are expanded compared with main sequence stars of the same mass as a consequence of unusually high mass transfer rates and/or pre-CV nuclear evolution. We show that the location of the secondaries of all well-studied CVs in the spectral type period diagram implies that they are consistent with having near-solar metallicities. We show, furthermore, that the surface brightness of K/M stars depends on gravity and metallicity and present new Barnes-Evans relations valid for dwarfs of near-solar metallicity and the secondaries in CVs of the galactic disk population. Distances derived by the surface brightness method agree with recent measurements of the trigonometric parallaxes of a few selected systems.

## 1. Are the secondary stars in CVs main sequence stars?

The secondary stars in CVs have been recognised to follow approximately the mass–radius relation of main sequence field stars [Echeverría, 1983, Patterson, 1984, Warner 1995, Smith & Dhillon, 1998]. A detailed comparison is complicated by the lack of information both on the masses of the secondary stars in CVs and of the masses and radii of main sequence field stars. It is advantageous, therefore, to restrict the comparison to quantities readily observable in CVs, as the orbital period  $P$  and the spectral type  $Sp$  of the secondary star [Beuermann et al., 1998, henceforth BBKW98, Smith & Dhillon, 1998]. This approach requires to construct an equivalent diagram for field stars predicting the orbital period of a CV at which a field star of given spectral type would fill the Roche-lobe of the secondary. Note that this prediction is almost independent of the mass of the white dwarf primary.

Figure 1 shows the spectral types of the secondaries in CVs with known orbital period. The data points are based on published optical/near-IR spectra quoted in the compilation of Ritter & Kolb [1998] with some recent spectral type determinations added [e.g., Schwarz et al., 1999, Smith et al., 1999, Thomas et al., 1999, Thorstensen et al., 1999]. Purely photometric spectral type assignments have not been included. We have also not included spectral types derived from IR spectra only.

Constructing a spectral type period diagram for field stars requires knowledge of their masses and radii. Unfortunately, both quantities are not generally well known. In this situation it is important to note that recent progress in the construction of stellar models [Baraffe et al., 1998, henceforth BCAH98] combined with the *NextGen* model atmospheres of Hauschildt et al. [1999] have led to a substantially improved definition of the lower main sequence [Leggett et al., 1996, henceforth L96]. In fact, as noted by BBKW98,

<sup>1</sup>Research supported in part by the Bundesministerium für Bildung und Wissenschaft under BMBF/DLR grant No. 50 OR 9210.

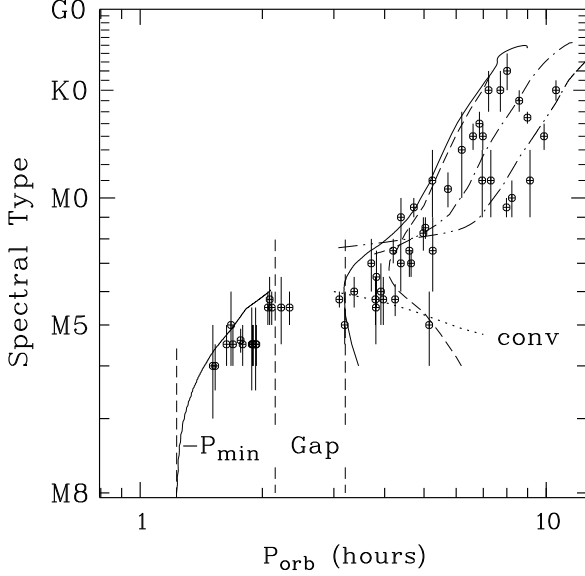


Fig. 1. Spectral types of CVs as a function of orbital period. The theoretical curves are from BBKW98 and Kolb & Baraffe [1999].

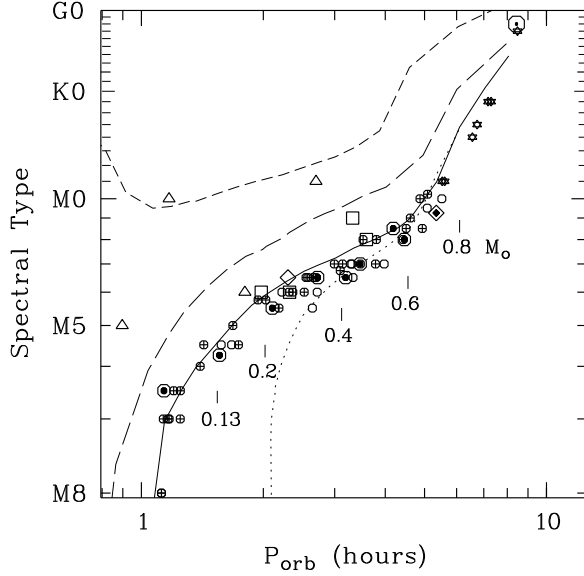


Fig. 2. Spectral type orbital period distribution for field stars assumed to be Roche-lobe filling secondaries in CVs. See text for explanation of symbols and theoretical curves [BCAH98].

the theoretical and observational radii of M-stars [L96] agree at the few % level for stars of given absolute  $K$ -band magnitude  $M_K$ . Using the observed radii, we have established a radius scale which allows to estimate the radii of field stars of given  $M_K$  [Beuermann et al., 1999, henceforth BBH99]. For the present purpose, we adopt the same stellar models which accurately reproduce the radii to estimate the masses, too. Specifically, we use the theoretical relation between mass and absolute  $K$ -band magnitude,  $M(M_K)$  [BCAH98] to calculate the above defined ‘orbital period’ for a field star of known  $M_K$  and  $Sp$ . We do not follow the approach of Clemens et al. [1998] who adopted the observational relation between mass and absolute magnitude of Henry & McCarthy [1993] because this relation represents a mean for stars of different age and metallicity and we want to study how differences in metallicity affect the location of stars in the  $Sp - P$  diagram.

Figure 2 shows the resulting  $Sp - P$  diagram for field stars of spectral types K/M supplemented by the Sun. The main sequence of stars with near-solar metallicity is delineated by eight young disk (YD) field stars from L96 (●), the YD binary YY Gem (◆), the Sun (○), and further 56 stars (★, ○, ⊕) with radii from [BBH99]. The effects of decreasing metallicity are indicated by the binary CM Dra (◇) and by four old disk stars (□) and four halo stars (△) from L96. Also shown in Fig. 2 are the models curves from the BCAH98 stellar models, namely the ZAMS model for solar metallicity (solid line), and models for stars aged  $10^{10}$  yrs with 1/3 solar metallicity (long dashes) and 1/30 solar metallicity (short dashes). For the model stars, the spectral type is assigned by converting the theoretical colour  $I - K$  to  $Sp$  [BBKW98]. The solid curve is expected to agree with the locus of the late-type YD stars. The slight displacement is probably due to remaining errors in the transformations used.

Comparison with Fig. 1 indicates that the (zero age) main sequence of low-mass field stars with near-

solar metallicity coincides with the locus of CV secondaries of the earliest spectral types at any given value of  $P$ . The upper left in Fig. 1 is devoid of CVs and shows that none of the systems included in the figure contains a secondary with metallicity substantially lower than the Sun (larger than solar metallicities are not excluded but remain unproven at present). The low space density of Pop II CVs is in agreement with population studies by Stehle et al. [1999]. The secondaries in many CVs with  $P > 3$  h have a later spectral type than expected for ZAMS secondary stars of near-solar metallicity. These secondaries are expanded over and have lower masses than Roche-lobe filling ZAMS stars. The two principal causes for this expansion are the loss of thermal equilibrium due to the on-going mass transfer and nuclear evolution prior to the onset of Roche-lobe overflow. Kolb & Baraffe [1999] have computed corresponding evolutionary sequences which nicely explain the observed behaviour and of which first results were presented in BBKW98. The paths included in Fig. 2 refer to secondaries starting as ZAMS stars of  $1 M_{\odot}$  and evolving under mass loss rates of  $1.5 \times 10^{-9} M_{\odot} \text{ yr}^{-1}$  (solid curve) and  $5 \times 10^{-9} M_{\odot} \text{ yr}^{-1}$  (dashed curve). The point on these paths where the secondary becomes fully convective is indicated by the dotted curve [Kolb & Baraffe, 1999]. Late spectral types in CVs with orbital periods between 3 and 5 h can be explained by this scenario. The evolutionary models suggest that whenever the secondary becomes convective it has reached  $\sim 0.2 M_{\odot}$  and  $Sp \sim M4.5$ . If angular momentum loss drops rapidly at this point the secondary enters the period gap and reappears below the gap with the same mass and spectral type  $Sp \sim M4.5$ . The comparatively late spectral types in CVs with orbital periods larger than 5 h can not be explained by the loss of thermal equilibrium due to mass loss but are consistent with nuclear evolution of the secondary star prior to the onset of mass transfer. Two evolutionary paths are included in Fig. 2 for secondaries starting mass transfer at  $M = 1 M_{\odot}$  with a rate of  $1.5 \times 10^{-9} M_{\odot} \text{ yr}^{-1}$  and a central hydrogen fraction which is reduced to 0.16 (dot-dashed curve) or is practically exhausted (dot-dot-dashed curve) [BBKW98, Kolb & Baraffe, 1999]. Early evolutionary calculations of a similar type were performed by Whyte & Eggleton [1980].

The model calculations of Kolb & Baraffe [1999] indicate that stars driven out of thermal equilibrium stay at approximately the same effective temperature and spectral type as an undisturbed star of the same mass. Their results allow to estimate the masses of the secondary stars and thereby their Roche radii from the observed spectral types. This is a prerequisite for distance determinations of CVs using the surface brightness method [Bailey 1981].

## 2. The brightness distribution of CV secondaries

The Roche-lobe filling secondary stars experience gravity darkening and will not be of uniform surface brightness. More seriously and more difficult to model are the variations in surface brightness caused by irradiation. Marsh [1990] showed that the strengths of the TiO bands and the NaI $\lambda\lambda 8183, 8195$  absorption-line doublet decrease on the hemisphere of the M5 secondary star in HT Cas which faces the primary. Naively, one might expect that heating of the secondary star produces an earlier spectral type and a corresponding increase in the TiO band strength. Observation indicates an opposite result, a decreased flux of the TiO features on the illuminated hemisphere, which suggests that a major change in the atmospheric structure takes place as a result of heating. Schwone et al. [1999] present a nice tomographic picture of the non-uniform appearance of the secondary star of QQ Vul in the NaI lines. Similar results have been obtained e.g. for AM Her [Southwell et al., 1995], illustrating the complications caused by the non-uniform appearance of the secondary star for dynamic mass determinations. This non-uniformity must be taken into account when applying the surface brightness method for distance measurements.

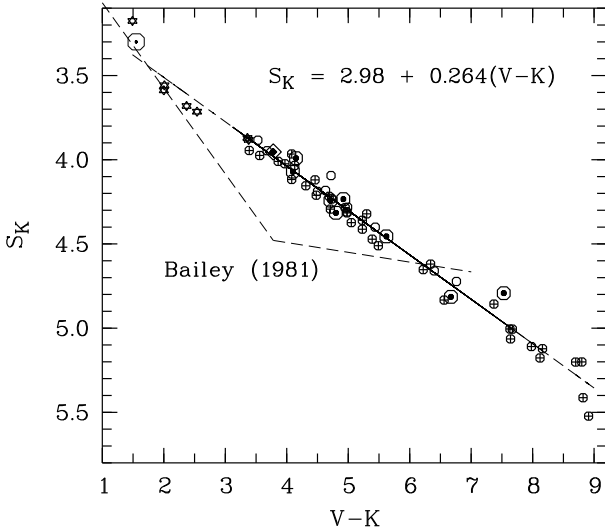


Fig. 3. Surface brightness  $S_K$  in the  $K$ -band as a function of colour  $V - K$  for single field stars with near-solar metallicity.

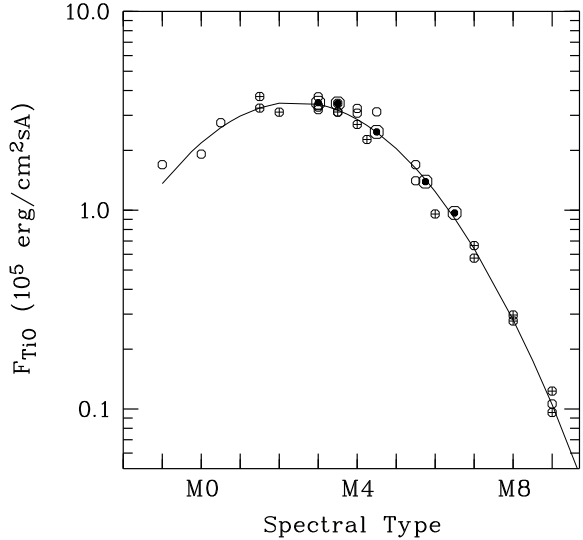


Fig. 4. Surface brightness  $T_{TiO}$  (in  $10^5 \text{ erg cm}^{-2}\text{s}^{-1}$ ) as a function of spectral type  $Sp$ .

### 3. Barnes-Evans relation for field M-dwarfs

Barnes & Evans [1976] found that the visual surface brightness of giants and supergiants (the only stars for which directly measured radii are available, apart from the few eclipsing binaries) is a function of colour only and independent of luminosity (gravity). BBH99 derived the surface brightness for the M-dwarfs studied by L96 and demonstrated that it deviates from that of giants. The implied small gravity dependence is in perfect agreement with recent model calculations for dwarfs and giants [BCAH98, Hauschildt et al., 1999]. The dwarf/giant difference reaches a maximum for  $Sp \simeq M0$  ( $V - I_c = 1.7$ ,  $V - K = 3.5$ ). BBH99 also showed that the surface brightness of dwarfs in the  $K$ -band depends on metallicity in agreement with the predictions of BCAH98. Since the well-observed CVs have near-solar metallicities (Figs. 1 and 2), consideration of the gravity and metallicity dependencies allows improved surface brightness-colour relations to be established which are valid, e.g., for CVs of the galactic disk population. Fig. 3 shows the resulting surface brightness  $S_K$  in the  $K$ -band as a function of colour  $V - K$  which can be fit by the linear relationship given in the figure. This relation differs from the original relation of Bailey [1981] which was widely used in CV research. Bailey's calibration of  $S_K$  depended on the Barnes-Evans relation for giants and is, therefore, expected to be low by some 0.3-0.4 mag near spectral type M0 or  $V - K = 3.5$ . The systematic difference between the two relations is primarily due to the gravity dependence of  $S_K$ . The often-cited near constancy of  $S_K$  for M-dwarfs does not exist. The scatter in our data is substantially reduced over that in Bailey's diagram, and in the similar one by Ramseyer [1994], because we considered only single dwarfs with near-solar metallicity and avoided colour transformations between different photometric systems. Low-metallicity M-dwarfs have  $S_K$  values lower by  $\sim 0.5$  mag. There is a systematic uncertainty in the derived surface brightness of about 0.1 mag carried over from the remaining uncertainty in the radius scale [BBH99].

The secure identification of CV secondary stars requires spectroscopic observations in the optical/near-

Table 1

Distances of CVs determined from the strength of the  $\text{TiO}\lambda 7500, 7165$  band strength, the  $K$ -magnitude of the secondary and compared with trigonometric parallaxes. The distances scale with secondary mass  $M_2$  as  $M_2^{1/3}$ .

Name	$P_h$	$Sp$	$f_{\text{TiO}}$	$K$	$M_2/M_\odot$	$d_{\text{pc}}(f_{\text{TiO}})$	$d_{\text{pc}}(K)$	$1/\pi$
<i>(1) The clear cases :</i>								
V834Cen	1.69	M5.5	1.78	13.85	0.13	$113 \pm 16$	$111 \pm 9$	
Z Cha	1.79	M5.5	1.27	14.05	0.13	$128 \pm 18$	$117 \pm 10$	
AM Her	3.09	M4+	21.0	11.71	0.27	$81 \pm 7$	$90 \pm 7$	$85 \pm 5$
U Gem	4.25	M4+	37.0	10.91	0.41	$88 \pm 11$	$92 \pm 7$	$96 \pm 4$
<i>(2) Some hopefully clear cases :</i>								
BL Hyi	1.89	M5.5	1.13	—	0.16	$163 \pm 23$		
RX0203	1.89	M2.5	1.10	—	0.45	$630 \pm 60$		
UZ For	2.11	M4.5	0.89	—	0.20	$263 \pm 29$		
TT Ari	3.30	M3.5	2.20	—	0.30	$297 \pm 25$		
IX Vel	4.66	M2?	—	10.7	0.50		$103 \pm 12$	$96 \pm 9$
AE Aqr	9.88	K4	—	$> 8.73$	0.50		$> 87 \pm 10$	$102 \pm 32$
<i>(3) Some controversial cases :</i>								
HT Cas	1.77	M5.4	0.98	15.4 :	0.13	$150 \pm 15$	$> 215$	
SS Cyg	6.60	K4	—	10.2 :	0.70	—	$152 \pm 15$ :	$166 \pm 13$
V1309 Ori	7.98	M0.5	1.09	$> 15.5$	0.45	$745 \pm 70$	$> 1370$	

IR spectral regions. M-stars are best detected by their pronounced TiO bands in the red part of the optical spectrum which display a variation in band strength ratios with spectral type [Wade & Horne, 1988, Marsh, 1990]. We have calibrated the *absolute strength* of the flux depression at  $7165\text{\AA}$  relative to the quasi-continuum at  $7500\text{\AA}$  vs. spectral type for a selection of field stars with near-solar metallicities and show the result in Fig. 4. The quantity  $F_{\text{TiO}} = (F_{\lambda 7500} - F_{\lambda 7165}) \times d^2/R^2$  is the TiO flux depression expressed as a surface brightness, with  $d$  the distance and  $R$  the stellar radius. The spectral fluxes  $F_{\lambda 7500}$  and  $F_{\lambda 7165}$  represent averages over  $\pm 50$  and  $\pm 25\text{\AA}$ , respectively. Different from the surface brightness  $S_K$  above,  $F_{\text{TiO}}$  is given in physical units. A second order polynomial fit to the logarithm of  $F_{\text{TiO}}$  is

$$F_{\text{TiO}} = 10^{5+\alpha} \text{ erg cm}^{-2}\text{s}^{-1}\text{\AA}^{-1} \quad \text{with} \quad \alpha = -1.477 + 0.5332(10 - S) - 0.03516(10 - S)^2 \quad (1)$$

where  $S$  is the spectral subtype for M-dwarfs, i.e.  $S = 5.5$  for an dM5.5 secondary, and  $S = -1$  for K7, preceding M0. Eq. (1) is applicable to all CVs which have secondaries with near-solar abundances. For metal-poor M-dwarfs of the old-disk and halo populations, the surface brightness  $F_{\text{TiO}}$  is reduced over that of Eq. (1). In extreme subdwarfs the  $\lambda 7165$  flux depression disappears and our definition of  $F_{\text{TiO}}$  becomes meaningless. Hence, Eq. (1) needs revision should spectral types become available for the secondaries in Pop II CVs, e.g., in globular clusters.

#### 4. Distance measurements of CVs

The surface brightness method [Bailey, 1981] allows the measurement of distances of CVs if the  $K$ -band flux of the secondary star or its spectral flux in the  $\text{TiO}\lambda 7500, 7165$  band can be measured. To be sure, the secondaries in CVs display a non-uniform surface brightness and care should be taken if

only a single spectrum or flux measurement are available. Ideally, the full orbital modulation is needed in order to select the most appropriate view on the secondary star for comparison with the appropriate surface brightness of field stars. In general, the  $K$ -band fluxes are not seriously affected by irradiation, while spectral features as the TiO bands and the NaI absorption lines are greatly diminished in strength on the heated face of the secondary star [e.g. Marsh, 1990, Schwope et al., 1999]. Both methods have, therefore, advantages and disadvantages. The advantage of using the TiO band strength lies in its easy identification in observed spectra.

We have used both the  $K$ -band brightness of the secondary and its TiO band strength to derive the distances of selected CVs and show some results in Table 1 (for a more detailed discussion see Beuermann & Weichhold, 1999. Note that the error in  $M_2$  has not been considered and the distances scale as  $M_2^{1/3}$ ). Ideally, both methods should yield the same distances which should agree within errors with the trigonometric parallax. This is, in fact, the case for of AM Her and U Gem (parallaxes by C. Dahn, private communication, Harrison et al., 1999). We have confidence also in the distances derived for V834 Cen and Z Cha which have no trigonometric parallaxes yet. There are some hopefully clear cases which represent CVs with well-defined TiO features. Obtaining independent distance information for these systems, e.g., from the  $K$ -band fluxes of the secondary stars is clearly desirable. There are also controversial cases, however, which indicate some of the pitfalls of the methods. For HT Cas, the distance derived from infrared photometry (Berriman et al., 1987) is probably wrong, as noted already by Ramseyer [1994]. Another important case is that of SS Cyg which has  $K = 9.4$  in quiescence. If that IR flux is entirely due to the K4 secondary, as assumed by Bailey [1981], our calibration yields  $d = 105$  pc. On the other hand, the secondary contributes only about  $\sim 50\%$  of the visual flux which implies that it is has  $K \simeq 10.2$  and raises the distance to  $d \simeq 152$  pc, consistent with the recent HST FGS parallax of 166 pc [Harrison et al., 1999]. Note that assuming a K5 secondary would reduce  $d$  again to 133 pc. Finally, the 8-h AM Herculis binary V1309 Ori has an (evolved) M0–M1 secondary and a TiO distance of 745 pc. The optical flux and spectral type imply that the secondary accounts for most of the  $K$ -band flux which is inconsistent with the statement of Harrop-Allin et al. [1997] of a contribution as low as  $\sim 20\%$  based on  $K$ -band spectroscopy of the illuminated face of the secondary. The discrepancy is likely due to problems associated with the interpretation of illuminated stellar atmospheres.

We conclude that reliable distances of CVs can be obtained from both the  $K$ -magnitude and the TiO band strength of the secondary if its flux contribution can be unequivocally determined, illumination effects are taken properly into account, and the viewing direction on to the secondary is known. Measuring accurate distances to CVs allows to derive basic quantities as their absolute magnitudes and the mass transfer rates [Warner, 1987]. Much of our understanding of the physics of CVs [Warner, 1995] is based on the tedious derivation of such quantities.

## 5. Acknowledgements

I thank Isabelle Baraffe and Ulrich Kolb for many discussions and for allowing me to show their evolutionary paths in Fig. 1 prior to publication, Hans Ritter for pointing out some errors in my earlier compilation of spectral types of secondary stars, and Marc Weichhold for the initial work on this subject.

## References

- Baraffe I., Chabrier G., Allard F., Hauschildt P.H., 1998, A&A 337, 403 (BCAH98).
- Barnes T.G., Evans D.S., 1976, MNRAS 174, 489.
- Bailey J., 1981, MNRAS 197, 31.
- Berriman, G., Kenyon, S., Boyle, C., 1987, AJ 94, 1291
- Beuermann, K., Weichhold, M., 1999, A&A, in preparation
- Beuermann K., Baraffe I., Hauschildt, P., 1999, A&A, in press (BBH99).

Beuermann K., Baraffe I., Kolb U., Weichhold M., 1998, A&A 339, 518 (BBKW98).

Clemens J.C., Reid I.N., Gizis J.E., O'Brien M.S., 1998, ApJ 496, 392.

Echeverría J., 1983, Rev.Mex.Astron.Astrof. 8, 109.

Harrison T.E., McNamara B.J., Szkody P., McArthur, B.E., Benedict, G.F., Klemola, A.R., Gilliland, R.L., 1999, ApJ 515, L93.

Harrop-Allin, M.K., Cropper, M., Potter, S.B., Dhillon, V.S., Howell, S.B., 1997, MNRAS 288, 1033.

Hauschildt P.H., Allard F., Baron E., 1999, ApJ 512, 377. (*NextGen* models).

Henry T.J., McCarthy Jr. W., 1993, AJ 106, 773.

Kolb, U., Baraffe I., 1999, submitted to MNRAS.

Leggett S.K., Allard F., Berriman G., Dahn C.C., Hauschildt P.H., 1996, ApJS 104, 117 (L96).

Marsh T., 1990, ApJ 357, 621.

Patterson J., 1984, ApJS 54, 443.

Ramseyer T., 1994, ApJ 425, 243.

Ritter H., Kolb U., 1998, A&A 129, 83.

Schwarz R., Schwope A.D., Beuermann K. et al., 1998, A&A 338, 465 (Polar RX J0203+29).

Schwope A.D., Beuermann K., Catalán, M.S., Metzner, A., Smith, R.C., Steeghs, D., 1999, A&A in press (QQ Vul).

Smith D.A., Dhillon V.S., 1998, MNRAS 301, 767.

Smith R.C., Hawkins, N.A., Mehes, O., 1999, this conference.

Southwell K.A., Still M.D., Smith R.C., Martin J.S., 1995, A&A 302, 90.

Stehle R., Kolb U., Ritter H., 1999, MNRAS in press.

Thomas, H.-C., Beuermann, K., Burwitz, V., Reinsch, K., Schwope, A.D., 1999, A&A, submitted (Polar RX J1313-32).

Thorstensen, J.R., Taylor, C.J., Kemp, J., 1999, this conference.

Wade R.A., Horne K., 1988, ApJ 324, 411.

Warner, B., 1987, MNRAS 227, 23.

Warner B., 1995, Cataclysmic Variable Stars, Cambridge Astrophysics Series 28, (Cambridge: CUP).

Whyte C., Eggleton P., 1980, MNRAS 190, 801.